Direct Electro Plasmonic and Optic Modulation via a Nanoscopic Electron Reservoir

Wancong Li,* Qiang Zhou,* Pu Zhang,† and Xue-Wen Chen‡
School of Physics and Wuhan National Laboratory for Optoelectronics, Huazhong University of Science and Technology, Luoyu Road 1037, Wuhan 430074, China
and Institute for Quantum Science and Engineering, Huazhong University of Science and Technology, Luoyu Road 1037, Wuhan 430074, China

(Received 21 December 2021; accepted 26 April 2022; published 23 May 2022)

Direct electrical tuning of localized plasmons at optical frequencies boasts the fascinating prospects of being ultrafast and energy efficient and having an ultrasmall footprint. However, the prospects are obscured by the grand challenge of effectively modulating the very large number of conduction electrons in three-dimensional metallic structures. Here we propose the concept of nanoscopic electron reservoir (NER) for direct electro plasmonic and electro-optic modulation. A NER is a few-to-ten-nanometer size metal feature on a metal host and supports a localized plasmon mode. We provide a general guideline to construct highly electrically susceptible NERs and theoretically demonstrate pronounced direct electrical tuning of the plasmon mode by exploiting the nonclassical effects of conduction electrons. Moreover, we show the electro-plasmonic tuning can be efficiently translated into modulation of optical scattering by utilizing the antenna effect of the metal host for the NER. Our work extends the landscape of electro plasmonic modulation and opens appealing new opportunities for quantum plasmonics.

DOI: 10.1103/PhysRevLett.128.217401

Introduction.—Plasmonics with metallic nanostructures lies at the nexus of photonics, electronics, and nanotechnology [1]. By exploiting conduction electrons at a metal surface, the diffraction limit of light can be overcome, promising the miniaturization of many functional photonic devices and their integration with microelectronics on one chip [1–5]. Along this line, there is a key need to devise fast electrically tunable plasmonic systems or modulators for dynamic control and data transimission [1,6]. Indeed, active plasmonics has flourished with the development of various dynamic tuning schemes and applications [7–11]. To enable electrical reconfigurability, there are basically two classes of approaches, i.e., indirect approaches through changing the dielectric environment adjacent to the plasmonic element and direct schemes via modifying the metal properties. The indirect approaches rely on the susceptibility of the dielectric material to the external stimulus and have been applied for electro-optic modulators with outstanding performance [12], although they often require quite a long propagation path to accumulate appreciable changes. Compared with indirect approaches, direct plasmon tuning could have a smaller footprint and be in principle much faster since it is only the free electrons involved [13]. However, in practice, direct electrical tuning at optical frequency is a grand challenge because the very large number of conduction electrons in metals can hardly be maneuvered to a considerable extent. To circumvent the difficulty, researchers have used electrochemical means for plasmonic nanoparticles submerged in an ionic environment [14,15] and explored few-nanometre-thick metal films [16]. While impressively flexible plasmon tunings have been demonstrated along with interesting potential applications, their tuning speed is quite limited. Recently, the electron tunneling effect in tunneling junction structures has been studied toward electrically modulated nanoscale plasmon sources [17–19] or absorbers [9]. For such schemes based on quantum tunneling, ultrathin gaps are often required to ensure an appreciable tunneling current and ultrafast response might be obscured by the *RC* time in practice.

Here we introduce the concept of the nanoscopic electron reservoir (NER) for ultrafast and efficient direct electro plasmonic tuning and then theoretically show electro-optic modulation for three dimensional (3D) nanoantenna structures. A NER consists of a few-to-ten-nanometer size metal feature on a metal host and supports a highly localized plasmon mode. At such a scale length, conduction electrons exhibit significant nonclassical effects, including electron nonlocality [20–22], spillover [23,24], and Landau damping [25,26], which are often considered detrimental to the performance of designed plasmonic devices [21,25,27]. Here surprisingly, these nonclassical effects are harnessed to enable ultrafast and energy-efficient electric modulation. We illustrate firstly the material effect with one-dimensional (1D) structures and then the geometrical effect with 3D structures on the electro plasmonic tunability. To convincingly reveal the effects, we perform rigorous calculations based on density functional theory (DFT) for 1D systems and develop a refined quantum hydrodynamic model (QHDM) [26,28,29] for noble metals

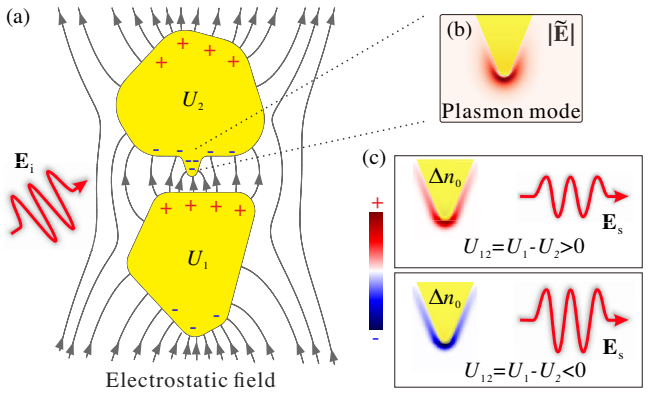

FIG. 1. (a) Schematic illustration of electro plasmonic and optic modulation via a NER situated on a metal host. The black arrowed lines represent the electrostatic field lines under an applied field $\mathbf{E}_c$, where U_1 and U_2 are the resulting potentials. (b) Plasmon mode field profile associated with the NER. (c) Change of the stationary conduction electron distribution Δn_0 varies with U_{12}. Δn_0 affects the plasmon mode and system far-field scattering. The red wavy lines with $\mathbf{E}_i$ and $\mathbf{E}_s$ denote the incident and scattering optical fields, respectively.

interfacing with dielectrics for 3D nanostructures. Finally we show that the pronounced electrical tuning of the plasmons can be translated into a deep modulation of the far-field scattering through the optical antenna effect of the host for the NER. We envision the present Letter will refresh the landscape of electro plasmonic tuning and bring appealing new opportunities for quantum plasmonics.

The concept.—The idea of the proposed electro plasmonic and -optic modulation is schematically illustrated in Fig. 1. The heart of Fig. 1(a) is a few-to-ten-nanometer feature at the bottom of the upper metal piece. The feature forms a NER and supports a localized plasmon mode, which is feasible since even atomistic protrusions can form isolated eigenmodes [30,31]. A typical plasmon mode profile is displayed in Fig. 1(b). The resonance depends on the stationary conduction electron density distribution $n_0(\mathbf{r})$, which could be modified by an applied electrostatic or low-frequency (compared with optical frequency) field, for instance with a bias voltage across the metallic dimer. Indeed, as shown in Fig. 1(c), the change of $n_0(\mathbf{r})$ could be prominent thanks to the small volume. Such electro plasmonic tuning is purely originated from nonclassical effects, out of which, the electron spill-out effect is the key [32]. By exploiting the antenna effect of the host on the NER [41], the change in the localized plasmon mode could be translated to the modification of system far-field response, i.e., modulation of the optical scattering. The electrical tunability of the NER mode is the key and depends on both the material and geometry of the structure.

Electrical tuning of electron distribution in 1D.—We perform a quantitative analysis of the material effect on the electrical tunability with a 1D configuration. The simple geometry allows us to reveal the critical roles of the

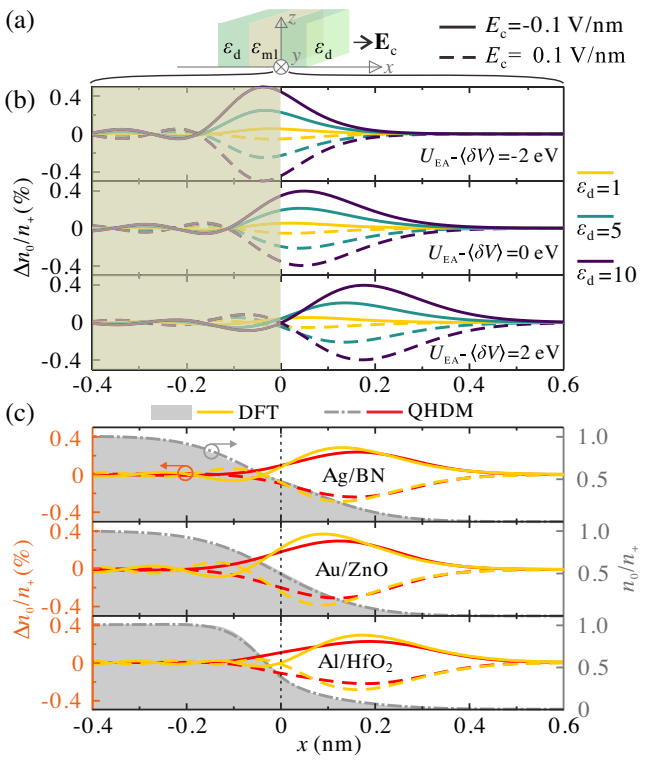

FIG. 2. (a) Sketch of the 1D configuration under study. (b) Calculated (DFT) position dependent $\Delta n_0/n_+$ for a variety of ε_d and $U_{\mathrm{EA}} - \langle \delta V \rangle$ (electron affinity difference of the metal and dielectric). (c) $\Delta n_0/n_+$ (left) and n_0/n_+ (right) for three metal-dielectric combinations. Results from DFT and our QHDM are both plotted.

interfacing materials' electron affinity and static permittivity in controlling the tunability by using rigorous DFT calculations based on a generalized jellium model [32,42,43]. It also serves as a benchmark for a refined QHDM we develop for noble metals in an applied bias field. As displayed in Fig. 2(a), the 1D system under study consists of a 5 nm thick metal slab embedded in a dielectric under an applied electrostatic field $\mathbf{E}_c$. The effect from the permittivity ε_d and electron affinity of the dielectric on the extent of electron spill over the metal-dielectric interface without $\mathbf{E}_c$ has been studied in the context of enhancing plasmonic absorption [44] and second-harmonic generation [45]. Here we investigate how the electrical tunability is affected by ε_d, the effective static permittivity due to metal's ion lattice $\varepsilon_{\mathrm{ml}}$, and the difference of the electron affinities between the dielectric and the metal's ion lattice. While the dielectric is known to have an electron affinity U_{EA}, the metal's ion lattice actually also has near-field effects describable by a pseudopotential $\langle \delta V \rangle$ [42], which effectively leads to an affinity difference of $U_{\mathrm{EA}} - \langle \delta V \rangle$ at the interface.

Fig. 2(b) presents the calculated stationary electron distribution change $\Delta n_0(\mathbf{r})$ [i.e., $n_0(\mathbf{r}, \mathbf{E}_c) - n_0(\mathbf{r}, \mathbf{E}_c = 0)$] normalized by the ion density in the metal n_+ as a function

of the position for a variety of $U_{\mathrm{EA}} - \langle \delta V \rangle$ and ε_d. Here we take silver as an example for the metal. All the plots show that Δn_0 grows with the increase of ε_d. However, the more important feature is the location of the maximum change. When $U_{\mathrm{EA}} - \langle \delta V \rangle$ is relatively low [cf. the first panel of Fig. 2(b)], $\Delta n_0(\mathbf{r})$ mainly resides inside the metal and will not provide good tunability to the plasmon mode since the small percentage change is on top of a large $n_0(\mathbf{r})$. Conversely, as the affinity difference increases and turns positive [cf. the third panel of Fig. 2(b)], the maximum $\Delta n_0(\mathbf{r})$ is out of the metal where $n_0(\mathbf{r})$ is much lower and therefore offers a high tunability. This important finding guides us to make appropriate metal-dielectric combinations. In Fig. 2(c), we demonstrate the properties of electron tunability for three workable combinations: Ag/BN(boron nitride), Au/ZnO, and Al/HfO_2. They all exhibit comparable maxima for $\Delta n_0(\mathbf{r})$ in regions with relatively low $n_0(\mathbf{r})$ (cf. gray shadings). Large electrical tunability thus could be expected. Next we focus on the Ag/BN combination and provide the results of other combinations in the Supplemental Material [32].

QHDM for noble metals under an applied bias.—While the DFT can conveniently treat the above 1D configurations, it becomes computationally impractical for 3D systems larger than a few nanometers. QHDMs are capable of efficiently describing the microscopic details of conduction electrons in a macroscopic system [26,28,29]. Good agreements between QHDM and DFT calculations have been recognized for simple metals like sodium [28,46]. However, for noble metals, their ion lattice containing bound electrons exerts near-field effects on the stationary distribution of conduction electrons that are not treated in usual QHDMs. Moreover, the present situation involves the metal interfaced with dielectrics in an applied field. There is no existing QHDM applicable, which motivates us to develop one. We separately treat the contributions of bound and conduction electrons [32]. The latter is described by the QHDM where the density distribution $n(\mathbf{r}, t)$ is perturbatively treated as $n(\mathbf{r}, t) = n_0(\mathbf{r}) + n_1(\mathbf{r}, t)$. $n_1(\mathbf{r}, t)$ is the optical response considered small relative to the stationary distribution $n_0(\mathbf{r})$. The essence of our development lies in rectifying $n_0(\mathbf{r})$ via the following set of modified QHDM equations for $f_{0,i} = \sqrt{n_{0,i}/n_{+,i}}$ and electrostatic potential ϕ:

$$\left(-\frac{\lambda_w \hbar^2}{2m}\nabla^2 + V_{\mathrm{eff}}\right) f_{0,i} = \mu_i f_{0,i}, \tag{1}$$

$$V_{\mathrm{eff}} = V_{\mathrm{int}} - U_{\mathrm{aff}} + q_e\phi + q_e\phi_{\mathrm{ext}}, \tag{2}$$

$$\nabla \cdot (\varepsilon_r \nabla \phi) = \frac{q_e}{\varepsilon_0}\sum_i (n_{+,i} - n_{0,i}), \tag{3}$$

where the subscript i denotes the ith metal piece in a system. The first term in Eq. (1) is the von Weizsäcker kinetic energy characterized with λ_w, and V_{int} in Eq. (2) is the interaction energy describing various nonlocal and quantum effects [26,28,29,32]. m, q_e, and μ_i are the electron mass, charge, and chemical potential of the metal [47], respectively. U_{aff} and ε_r concisely represent U_{EA} and ε_d in the dielectric, or $\langle \delta V \rangle$ and $\varepsilon_{\mathrm{ml}}$ in the metal, respectively. These two newly introduced ingredients effectively amend the QHDM by accounting for the near-field and polarization effects of the metal ion lattice (including bound electrons) and the dielectric. When $\mathbf{E}_c$ is applied, the external potential ϕ_{ext} is found from the homogeneous Poisson equation $\nabla \cdot (\varepsilon_r \nabla \phi_{\mathrm{ext}}) = 0$ with boundary condition $-\nabla \phi_{\mathrm{ext}}|_\infty = \mathbf{E}_c$. For a system consisting of two or more metal pieces, bias voltages instead of $\mathbf{E}_c$ may be more convenient to apply, and then ϕ_{ext} is set to zero. The chemical potentials μ_i are related to the applied voltages $\mu_i - \mu_j = q_e U_{ij}$.

In Fig. 2(c), $n_0(\mathbf{r})$ at $\mathbf{E}_c = 0$ and the change $\Delta n_0(\mathbf{r})$ with $\mathbf{E}_c$ from our QHDM are compared with the DFT calculations. In all cases, $n_0(\mathbf{r})$ distributions from QHDM (dash-dotted lines) in Fig. 2(c) perfectly match with the DFT results (shadings). In view of the small magnitudes of $\Delta n_0(\mathbf{r})$, the distributions obtained from our QHDM agree pretty well with the DFT results. Once $n_0(\mathbf{r})$ is obtained, the calculation of the optical response via QHDM follows from the established procedure [26,28,29]. The model parameters of our QHDM (including λ_W and Landau damping strength) for computing the stationary state and optical responses are respectively calibrated with (time-dependent) DFT by fitting the n_0 of a metal slab and nanoparticle resonances of simple metals [48]. The calibrated QHDM is further benchmarked with time-dependent DFT under jellium approximation within the package Octopus [49] for few-to-ten-nanometer particles of different shapes and materials (both simple and noble metals). Good agreements are obtained for all the studied cases [32,48].

Electro plasmonic tuning in 3D configurations.—We proceed to reveal the geometry effect of the NER based on our QHDM calculations and demonstrate direct electro plasmonic tuning. As sketched in Fig. 3(a), a generic structure, i.e., a 40 nm Ag nanosphere with a cone-shaped NER in the dielectric background of BN, is studied. The NER has a height H of 4 nm and a base diameter D. The radius of curvature at the tip apex is fixed to 1 nm, which is assumed for all NER structures studied in this Letter. The structure is subject to an electrostatic field $\mathbf{E}_c$, and the resulting field is intuitively illustrated by the lines. Figure 3(b) presents $\Delta n_0/n_+$ in the NER for $D = 4$ nm as E_c varies from -0.1 V/nm to 0.1 V/nm, which exhibits more and more electron spill out. Remarkably, here $\Delta n_0/n_+$ reaches $\pm 4\%$, an order of magnitude higher than in the 1D configuration. To reveal how these changes affect the plasmon mode associated with the NER, we perform quasinormal mode analysis [32,50–52] and show

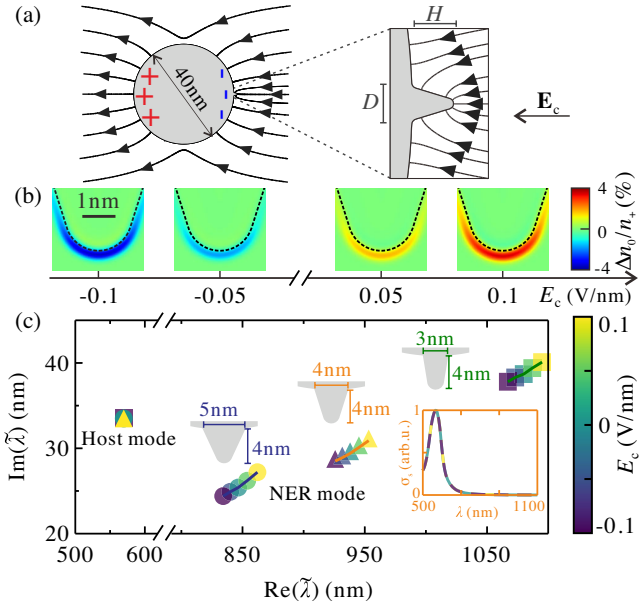

FIG. 3. Electro plasmonic tuning in 3D metallic configuration. (a) Schematic of a 40 nm Ag nanosphere with a conical NER characterized by the base D and height H. The nanosphere is under an external electrostatic field $\mathbf{E}_c$, and the black arrowed lines denote the field lines. (b) $\Delta n_0/n_+$ in the NER for various $\mathbf{E}_c$. The dotted lines indicate the metal boundary. (c) Evolution of the complex eigenwavelengths ($\tilde{\lambda}$) with E_c for three (D, H). Insets: far-field scattering spectra of the nanosphere with $D = H = 4$ nm at various E_c.

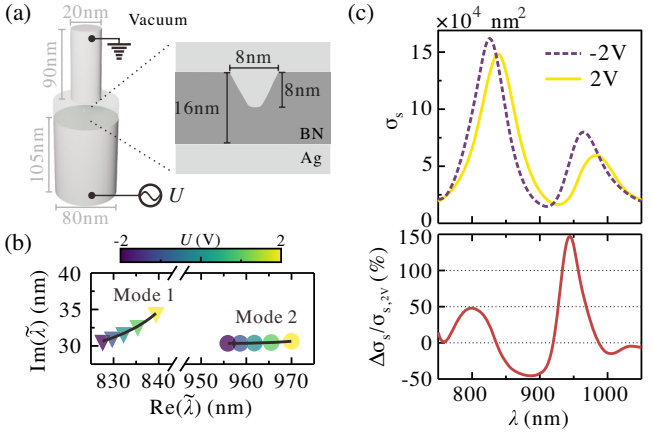

FIG. 4. Electro-optic modulation. (a) Schematics of the hybrid antenna with structural specifications. (b) Evolutions of the complex eigenwavelengths of the modes with the change of the bias voltage. (c) Top: spectra of far-field scattering cross sections (σ_s) for $U = 2$ V (solid) and -2 V (dashed). Bottom: spectrum of $(\sigma_{s,-2V} - \sigma_{s,2V})/\sigma_{s,2V}$ in percentage.

the evolution of the complex eigenwavelengths of the modes [32] with E_c in Fig. 3(c). Symbols of circles, triangles, and squares correspond to the modes of the structures with $D = 5$ nm, 4 nm, and 3 nm, respectively. The resonance at 569 nm is the dipolar mode of the nanosphere host and does not change with the applied field. In stark contrast, the plasmon mode associated with the NER exhibits remarkable electrical tunability. The resonant wavelength redshifts by about 30 nm for all D values as E_c varies from -0.1 V/nm to 0.1 V/nm. Further calculations show the shape of the NER regulates the resonant wavelength and its size influences the range of electro plasmonic tuning [32]. However, such pronounced electro plasmonic tunability is not necessarily observable from spectroscopic studies. The far-field scattering spectra for the $D = 4$ nm case under various E_c are depicted in the inset of Fig. 3(c) and exhibit negligible change due to the fact that the localized mode is nonradiative. The nonradiative nature and the electric tunability of the NER mode could also be probed by using a dipole emitter as the excitation source [32,53]. Our analysis by tracing the mode evolution helps us to grasp the intrinsic physics of plasmon tuning.

Electro-optic modulation.—The remaining task is to resolve the nonradiative problem of the NERs' plasmon mode and achieve electro-optic modulation. The problem has its root in the mismatch of the size of the mode with the free-space optical wavelength. Inspired by the idea of using optical antenna to enhance the spontaneous emission of an atom [41], we utilize the host body of the NER as an antenna to interface the far field and the NER mode. Similar principles have been employed to enhance the radiation of extremely localized modes [30,31,54], which are order-of-magnitude more localized than here. Here specifically, we devise a cylindrical heterodimer nanoantenna shown in Fig. 4(a) as the host for the NER in the BN gap. As sketched in Fig. 4(a), a 16 nm thick gap is used to enhance the radiation and avoid electron tunneling under a few-volt bias. Moreover, the dimer configuration admits a more convenient voltage based tuning. The cone-shaped NER has a much larger size than those studied in Fig. 3 in order to improve the coupling with the far field and for ease of fabrication and structural robustness by sacrificing a bit of tunability.

We perform quasinormal mode analysis for the whole system and show in Fig. 4(b) the evolution of the complex eigenwavelengths of its modes as the control voltage U varies from -2 V to 2 V. The system supports two eigenmodes (Mode 1 and 2) [32] as a result of strong coupling between the host and the NER. The optical modal field and $\Delta n_0(\mathbf{r})$ due to the applied voltage have good spatial overlap [32]. The radiation efficiency of the modes now could reach 20%, much larger than the efficiency of the NER mode in Fig. 3 [32]. Therefore, there should be pronounced far-field optical modulations although the tuning range is smaller than those of Fig. 3(c) as explained earlier. The upper panel of Fig. 4(c) displays the spectra of a far-field scattering cross section for two bias voltages of $U = -2$ and 2 V. The spectrum of relative change is plotted in the lower panel and exhibits a maximum achievable change of 150% near 944 nm with a full width of half

maximum of about 10 THz. Importantly, it is remarkably bright with a far-field scattering cross section of $\sigma_s = (230\ \mathrm{nm})^2$ for $U = -2$ V.

Discussion and summary.—We have theoretically shown that a nanoscopic electron reservoir formed on the surface of a metal host allows direct electrical tuning of its localized plasmon mode, which can be broadcast to the far field over a broad bandwidth. The origin of the direct tuning lies in that the stationary electron distribution $n_0(\mathbf{r})$ in the tiny reservoir is susceptible to the external electrical stimulus and determines its optical response. We reveal that the electrical tunability critically relies on the electron affinity difference and dielectric permittivity of the interfacing materials. We consequently provide a guideline to select appropriate combinations of metal-dielectric for nanoscopic electron reservoirs with plasmon modes highly susceptible to electrical stimulus.

There are a number of remarkable features in our finding. A key feature is the potential for ultrafast operation. The conduction electrons respond to electric field within $10 \sim 20$ femtoseconds (fs) considering their relaxation time. Meanwhile, considering the tiny footprint of the structure, the RC time of establishing the electric field could be less than 1 fs [32]. Thus a simple estimation of the time to form a changed $n_0(\mathbf{r})$ upon an electrical stimulus gives around 10–20 fs. We remark that a more sophisticated theory is certainly required to accurately describe the detailed dynamics [55]. Another accompanying crucial feature is the ultralow energy required for the modulation. In our scheme, there is no conduction or tunneling current since the gap is too large for tunneling [8 nm in Fig. 4(a)]. This is in stark contrast to the modulations involving inelastic electron tunneling [17–19], where the low electron-to-photon conversion efficiency requires a considerable tunneling current that consumes energy. Here, in our scheme, the electric signal does not generate light but only modulates the far-field scattering. For the tiny capacitance of our device, a simple estimation of the minimum energy consumption for one operation of changing 2 to -2 V is about 71 aJ [32,56,57]. An additional feature of our finding is the generality. The proposed electro plasmonic and -optic modulation could work for a variety of metal-dielectric material combinations and geometries [32]. It may also work for narrow magnetoplasmonic resonances associated with a cluster of metal nanoparticles [58]. The concerned structural features have dimensions of few to ten nanometers and are challenging but possible for deterministic fabrication [59–64]. Our theoretical finding opens up exciting applications of quantum plasmonics and stimulates new experiments.

We acknowledge financial support from the National Natural Science Foundation of China (Grants No. 9215011 and No. 11874166) and Huazhong University of Science and Technology. X.-W. C. would like to thank H. Duan for discussions on extreme nanofabrication. The computing work is supported by the public computing service platform provided by the Network and Computing Center of HUST.

*These authors contributed equally to this work.
†To whom all correspondence should be addressed. puzhang0702@hust.edu.cn
‡To whom all correspondence should be addressed. xuewen_chen@hust.edu.cn

[1] E. Ozbay, Plasmonics: Merging photonics and electronics at nanoscale dimensions, Science **311**, 189 (2006).
[2] P. Berini and I. De Leon, Surface plasmonpolariton amplifiers and lasers, Nat. Photonics **6**, 16 (2012).
[3] X. Guo, Y. Ma, Y. Wang, and L. Tong, Nanowire plasmonic waveguides, circuits and devices, Laser Photonics Rev. **7**, 855 (2013).
[4] W. Du, T. Wang, H.-S. Chu, and C. A. Nijhuis, Highly efficient on-chip direct electronicplasmonic transducers, Nat. Photonics **11**, 623 (2017).
[5] A. Dorodnyy, Y. Salamin, P. Ma, J. V. Plestina, N. Lassaline, D. Mikulik, P. Romero-Gomez, A. F. i. Morral, and J. Leuthold, Plasmonic photodetectors, IEEE J. Sel. Top. Quantum Electron. **24**, 1 (2018).
[6] L. Cao and M. L. Brongersma, Ultrafast developments, Nat. Photonics **3**, 12 (2009).
[7] A. V. Krasavin and N. I. Zheludev, Active plasmonics: Controlling signals in Au/Ga waveguide using nanoscale structural transformations, Appl. Phys. Lett. **84**, 1416 (2004).
[8] K. F. MacDonald, Z. L. Sámson, M. I. Stockman, and N. I. Zheludev, Ultrafast active plasmonics, Nat. Photonics **3**, 55 (2009).
[9] D. C. Marinica, M. Zapata, P. Nordlander, A. K. Kazansky, P. M. Echenique, J. Aizpurua, and A. G. Borisov, Active quantum plasmonics, Sci. Adv. **1**, e1501095 (2015).
[10] A. Habib, X. Zhu, S. Fong, and A. A. Yanik, Active plasmonic nanoantenna: An emerging toolbox from photonics to neuroscience, Nanophotonics **9**, 3805 (2020).
[11] N. Jiang, X. Zhuo, and J. Wang, Active plasmonics: Principles, structures, and applications, Chem. Rev. **118**, 3054 (2018).
[12] M. Ayata, Y. Fedoryshyn, W. Heni, B. Baeuerle, A. Josten, M. Zahner, U. Koch, Y. Salamin, C. Hoessbacher, C. Haffner, D. L. Elder, L. R. Dalton, and J. Leuthold, High-speed plasmonic modulator in a single metal layer, Science **358**, 630 (2017).
[13] M. I. Stockman, Ultrafast nanoplasmonics under coherent control, New J. Phys. **10**, 025031 (2008).
[14] L.-H. Shao, M. Ruther, S. Linden, S. Essig, K. Busch, J. Weissmüller, and M. Wegener, Electrochemical modulation of photonic metamaterials, Adv. Mater. **22**, 5173 (2010).
[15] A. M. Brown, M. T. Sheldon, and H. A. Atwater, Electrochemical tuning of the dielectric function of Au nanoparticles, ACS Photonics **2**, 459 (2015).
[16] R. A. Maniyara, D. Rodrigo, R. Yu, J. Canet-Ferrer, D. S. Ghosh, R. Yongsunthon, D. E. Baker, A. Rezikyan,

F. J. García de Abajo, and V. Pruneri, Tunable plasmons in ultrathin metal films, Nat. Photonics **13**, 328 (2019).
[17] J. Kern, R. Kullock, J. Prangsma, M. Emmerling, M. Kamp, and B. Hecht, Electrically driven optical antennas, Nat. Photonics **9**, 582 (2015).
[18] M. Parzefall, P. Bharadwaj, A. Jain, T. Taniguchi, K. Watanabe, and L. Novotny, Antenna-coupled photon emission from hexagonal boron nitride tunnel junctions, Nat. Nanotechnol. **10**, 1058 (2015).
[19] C. Zhang, J. P. Hugonin, A. L. Coutrot, C. Sauvan, F. Marquier, and J. J. Greffet, Antenna surface plasmon emission by inelastic tunneling, Nat. Commun. **10**, 4949 (2019).
[20] S. Raza, G. Toscano, A.-P. Jauho, M. Wubs, and N. A. Mortensen, Unusual resonances in nanoplasmonic structures due to nonlocal response, Phys. Rev. B **84**, 121412(R) (2011).
[21] C. Ciracì, R. T. Hill, J. J. Mock, Y. Urzhumov, A. I. Fernández-Domínguez, S. A. Maier, J. B. Pendry, A. Chilkoti, and D. R. Smith, Probing the ultimate limits of plasmonic enhancement, Science **337**, 1072 (2012).
[22] T. Christensen, W. Yan, S. Raza, A.-P. Jauho, N. A. Mortensen, and M. Wubs, Nonlocal response of metallic nanospheres probed by light, electrons, and atoms, ACS Nano **8**, 1745 (2014).
[23] C. David and F. J. García de Abajo, Surface plasmon dependence on the electron density profile at metal surfaces, ACS Nano **8**, 9558 (2014).
[24] W. Zhu, R. Esteban, A. G. Borisov, J. J. Baumberg, P. Nordlander, H. J. Lezec, J. Aizpurua, and K. B. Crozier, Quantum mechanical effects in plasmonic structures with subnanometre gaps, Nat. Commun. **7**, 11495 (2016).
[25] J. Khurgin, W.-Y. Tsai, D. P. Tsai, and G. Sun, Landau damping and limit to field confinement and enhancement in plasmonic dimers, ACS Photonics **4**, 2871 (2017).
[26] C. Ciracì, Current-dependent potential for nonlocal absorption in quantum hydrodynamic theory, Phys. Rev. B **95**, 245434 (2017).
[27] H. Hu, X. Lin, J. Zhang, D. Liu, P. Genevet, B. Zhang, and Y. Luo, Nonlocality induced cherenkov threshold, Laser Photonics Rev. **14**, 2000149 (2020).
[28] G. Toscano, J. Straubel, A. Kwiatkowski, C. Rockstuhl, F. Evers, H. Xu, N. A. Mortensen, and M. Wubs, Resonance shifts and spill-out effects in self-consistent hydrodynamic nanoplasmonics, Nat. Commun. **6**, 7132 (2015).
[29] K. Ding and C. T. Chan, Plasmonic modes of polygonal rods calculated using a quantum hydrodynamics method, Phys. Rev. B **96**, 125134 (2017).
[30] W. Li, Q. Zhou, P. Zhang, and X.-W. Chen, Bright Optical Eigenmode of 1 nm^3 Mode Volume, Phys. Rev. Lett. **126**, 257401 (2021).
[31] T. Wu, W. Yan, and P. Lalanne, Bright plasmons with cubic nanometer mode volumes through mode hybridization, ACS Photonics **8**, 307 (2021).
[32] See Supplemental Material at http://link.aps.org/supplemental/10.1103/PhysRevLett.128.217401 for the formulation of the refined QHDM and 1D DFT, details of numerical implementation, additional benchmark of QHDM and supporting results, which include Refs. [33–40].
[33] A. Liebsch, *Electronic Excitations at Metal Surfaces* (Springer, New York, 1997).
[34] V. Kulkarni, E. Prodan, and P. Nordlander, Quantum plasmonics: Optical properties of a nanomatryushka, Nano Lett. **13**, 5873 (2013).
[35] D. R. Lide, *CRC Handbook of Chemistry and Physics*, 87th ed. (CRC Press, Boca Raton, FL, 2006).
[36] L. J. Brillson, *An Essential Guide to Electronic Material Surfaces and Interfaces* (John Wiley & Sons, Ltd, New York, 2016).
[37] N. Del Fatti, C. Voisin, M. Achermann, S. Tzortzakis, D. Christofilos, and F. Vallée, Nonequilibrium electron dynamics in noble metals, Phys. Rev. B **61**, 16956 (2000).
[38] *Handbook of Optical Constants of Solids*, edited by E. D. Palik (Academic Press, Burlington, 1997).
[39] M. N. Polyanskiy, Refractive index database, https://refractiveindex.info (accessed on 2021-12-18).
[40] X.-W. Chen, V. Sandoghdar, and M. Agio, Nanofocusing radially-polarized beams for high-throughput funneling of optical energy to the near field, Opt. Express **18**, 10878 (2010).
[41] J.-J. Greffet, Nanoantennas for light emission, Science **308**, 1561 (2005).
[42] J. P. Perdew, H. Q. Tran, and E. D. Smith, Stabilized jellium: Structureless pseudopotential model for the cohesive and surface properties of metals, Phys. Rev. B **42**, 11627 (1990).
[43] Z. Yuan and S. Gao, Linear-response study of plasmon excitation in metallic thin films: Layer-dependent hybridization and dispersion, Phys. Rev. B **73**, 155411 (2006).
[44] D. Jin, Q. Hu, D. Neuhauser, F. von Cube, Y. Yang, R. Sachan, T. S. Luk, D. C. Bell, and N. X. Fang, Quantum-Spillover-Enhanced Surface-Plasmonic Absorption at the Interface of Silver and High-Index Dielectrics, Phys. Rev. Lett. **115**, 193901 (2015).
[45] M. Khalid and C. Ciracì, Enhancing second-harmonic generation with electron spill-out at metallic surfaces, Commun. Phys. **3**, 214 (2020).
[46] C. Ciracì and F. Della Sala, Quantum hydrodynamic theory for plasmonics: Impact of the electron density tail, Phys. Rev. B **93**, 205405 (2016).
[47] G. Manfredi, P.-A. Hervieux, and J. Hurst, Fluid descriptions of quantum plasmas, Rev. Mod. Plasma Phys. **5**, 7 (2021).
[48] Q. Zhou, W. Li, P. Zhang, and X.-W. Chen, Calibrating quantum hydrodynamic model for noble metals in nanoplasmonics, arXiv:2112.10099.
[49] N. Tancogne-Dejean *et al.*, Octopus, a computational framework for exploring light-driven phenomena and quantum dynamics in extended and finite systems, J. Chem. Phys. **152**, 124119 (2020).
[50] P. Lalanne, W. Yan, K. Vynck, C. Sauvan, and J. P. Hugonin, Light interaction with photonic and plasmonic resonances, Laser Photonics Rev. **12**, 1700113 (2018).
[51] P. T. Kristensen, K. Herrmann, F. Intravaia, and K. Busch, Modeling electromagnetic resonators using quasinormal modes, Adv. Opt. Photonics **12**, 612 (2020).
[52] Q. Zhou, P. Zhang, and X.-W. Chen, General Framework of Canonical Quasinormal Mode Analysis for Extreme Nano-Optics, Phys. Rev. Lett. **127**, 267401 (2021).
[53] P. A. D. Gonçalves, T. Christensen, N. Rivera, A.-P. Jauho, N. A. Mortensen, and M. Soljačić, Plasmon-emitter interactions at the nanoscale, Nat. Commun. **11**, 366 (2020).

[54] S. I. Bogdanov, O. A. Makarova, X. Xu, Z. O. Martin, A. S. Lagutchev, M. Olinde, D. Shah, S. N. Chowdhury, A. R. Gabidullin, I. A. Ryzhikov, I. A. Rodionov, A. V. Kildishev, S. I. Bozhevolnyi, A. Boltasseva, V. M. Shalaev, and J. B. Khurgin, Ultrafast quantum photonics enabled by coupling plasmonic nanocavities to strongly radiative antennas, Optica **7**, 463 (2020).

[55] T. Takeuci and K. Yabana, Numerical scheme for a nonlinear optical response of a metallic nanostructure: Quantum hydrodynamic theory solved by adopting an effective schrödinger equation, Opt. Express **30**, 11572 (2022).

[56] D. A. B. Miller, Energy consumption in optical modulators for interconnects, Opt. Express **20**, A293 (2012).

[57] M. de Cea, A. H. Atabaki, and R. J. Ram, Energy harvesting optical modulators with sub-attojoule per bit electrical energy consumption, Nat. Commun. **12**, 2326 (2021).

[58] A. Alù and N. Engheta, The quest for magnetic plasmons at optical frequencies, Opt. Express **17**, 5723 (2009).

[59] D. K. Oh, H. Jeong, J. Kim, Y. Kim, I. Kim, J. G. Ok, and J. Rho, Top-down nanofabrication approaches toward single-digit-nanometer scale structures, J. Mech. Sci. Tech. **35**, 837 (2021).

[60] V. R. Manfrinato, A. Stein, L. Zhang, C.-Y. Nam, K. G. Yager, E. A. Stach, and C. T. Black, Aberration-corrected electron beam lithography at the one nanometer length scale, Nano Lett. **17**, 4562 (2017).

[61] Y. Chen, Y. Hu, J. Zhao, Y. Deng, Z. Wang, X. Cheng, D. Lei, Y. Deng, and H. Duan, Topology optimization-based inverse design of plasmonic nanodimer with maximum near-field enhancement, Adv. Funct. Mater. **30**, 2000642 (2020).

[62] Y. Wang, M. Abb, S. A. Boden, J. Aizpurua, C. H. de Groot, and O. L. Muskens, Ultrafast nonlinear control of progressively loaded, single plasmonic nanoantennas fabricated using helium ion milling, Nano Lett. **13**, 5647 (2013).

[63] M.-K. Kim, H. Sim, S. J. Yoon, S.-H. Gong, C. W. Ahn, Y.-H. Cho, and Y.-H. Lee, Squeezing photons into a point-like space, Nano Lett. **15**, 4102 (2015).

[64] I. Kim, J. Mun, K. M. Baek, M. Kim, C. Hao, C.-W. Qiu, Y. S. Jung, and J. Rho, Cascade domino lithography for extreme photon squeezing, Mater. Today **39**, 89 (2020).